Mechanics and Mechanical Engineering
Vol. 10, No 1 (2006) 82–109

Plastic stresses, strains and the phase of failure in tension

Mieczysław Jaroniek
Technical University of Łódź,Department of Materials and Structures Strength
Stefanowskiego 1/15, 90-924 Łódź, Poland

Received (15 September 2006)
Revised (23 September 2006)
Accepted (3 October 2006)

In this paper the analysis of the state of strain and stress in necking has been analysed. A description of the stress-strain relationship, which takes into account strain hardening, and next necking until the moment of rupture, along with a description of breaking stresses, allows one to build such a mathematical model (described in bi-polar coordinates) in the whole range of load, which accounts for the fracture formation and the element failure.

Keywords: stress-strain relationship; bi-polar coordinates; moiré–fringe patterns; moiré method; finite element method

1. Introduction

In modern mechanical, building, structures, etc., an exact evaluation of the state of stresses and strains, possible failures of materials is needed both during their manufacturing and usage. Because of a complex nature of the material internal microstructure, local properties of the material that can propagate in time under the effect of heat and pressure, a local failure system, residual stresses caused by the technological process and other factors exert very often an influence on failure modes.

Results of experimental investigations are the basic element in formulation of theoretical solutions, however, despite a dynamic development in measuring techniques, an interpretation of test results can be difficult due to a limited spectrum and range of applicability of the apparatus used in tests. It seems that an application of latest calculation methods allows one to determine the boundary states and failure phases of a structure or an element on the basis of material properties. However, investigation methods are continuously modernised and the results of some research are protected by patents and made public unwillingly in numerous cases, thus such data should be supplemented with additional measurements, e.g., of strains in the failure phase, the determination of crack resistance, etc.

Strength resistance properties of materials are the basic element that enables calculations and formulation of theoretical solutions, however due to their limited spectrum in cases of complex stresses and strains, their explicit interpretation can be impeded.

As a classical example of such an approach, one can consider a simple tensile test as the basis for further calculations. The analysis of the failure phase under tension has been presented, for example, in [1], [4], [5], [17] and al.

Tension diagrams that characterize the material properties are treated as the fundamental element of numerical computations. Testing machines used currently allow one to describe precisely tensile tests, but their software enables the determination of only some parameters that define the material properties. The application of results of typical strength tests into numerical computations is incurred with errors that follow from the simplifications assumed. A lack of mathematical model, which would describe an actual $\sigma - \varepsilon$ (stress-strain) relationship in the whole range of load, compels designers to use simplified assumptions or to conduct additional recalculations in order to describe the complete tensile behaviour, including the failure phase. The investigations carried out by the author allow one to analyse subsequent tension phases, a failure mode and an occurrence of sliding planes and an actual $\sigma - \varepsilon$ relationship. The analysis of stress and strain states for St3s and St4s steel was made on an Instron testing machine. The displacement and strain measurements presented in this study were made with strain gauges, an extensometer and by means of the moiré-fringe technique [3, 6] and al.

In principle, strength tests on, e.g., an Instron testing machine, are carried out for two kinds of programs, namely:

1. Strain measurement is made with extensometers – then we can determine the proof stress or the physical yield point and the Young's modulus. Usually, when the proof stress or the physical yield point is exceeded, the extensometer should be turned off, and the strain recording program recalculates the jaw edge displacements and calculates the elongations as if they were still recorded by the extensometer, and next it calculates the tensile strength.

2. Strain measurement is made without extensometers – then we can determine the proof stress or the physical yield point and the tensile strength and elongations on the basis of a difference in displacements of the machine grip jaw edges.

A detailed analysis of such measurements is to be found in the next section of the present study.

The way the strains are described in bi-polar coordinates, which has been based on the experimental investigations, makes it possible to employ the results in the numerical computations, wherever we are interested in stress states in the failure phase. The real $\sigma - \varepsilon$ (stress-strain) relationship used in calculations (in elastic-plastic materials after strain hardening) comprises a description of strains until the moment of an occurrence of necking, next it describes a stress distribution after the occurrence of necking, and the process of fracture itself is described on the basis of tests of specimens with existing fissures.

The investigations of the fracture process and the analysis of causes of the scratch occurrence are the object of numerous scientific investigations and studies, and the complete range of methods and solutions, whose examples are listed at the end of this study, fall beyond the scope of the present study. In this study, some test and calculation methods that can be employed to develop a model of structures, which can be used in the engineering practice in the whole range of loading and which accounts for element fracture and failure investigations, have been presented. The tests were made on steel specimens and models made of epoxy resins with the linear characteristics (characterized by brittle cracking) and "elastic-plastic" resins (with the non-linear characteristics).

The numerical calculation results, and especially the finite element method, are now widely used in structure calculations.

The professional software packages (ANSYS, NASTRAN, ADINA) enable all kinds of computations, but the accuracy of these computations depends, among others, on the characteristics of structural materials, and thus on the data obtained in the basic investigations.

For instance, the professional ANSYS software allows for carrying out all kinds of computations. In this program in the range of elastic-plastic strains, the logarithmic stain $\overrightarrow{\varepsilon}$ is assumed instead of the conventional strain ε, and the value of the Poisson's ratio $\nu_{pl}(\varepsilon)$ is assumed as a constant and equal to 0.5, which agrees approximately with the real state of stresses and strains.

2. Results of tensile tests

The diagrams $\mathrm{F}(\Delta l)$ or $\sigma(\varepsilon)$ obtained from the testing machine should be interpreted so that the diagram $\sigma(\varepsilon)$ should correspond to real $\sigma - \varepsilon$ relationships. The characteristic quantities, on the basis of which the $\sigma - \varepsilon$ relationship can be formed, are the forces corresponding to the physical yield point or the proof stress, the maximum force and the strain corresponding to it, and the force acting when the specimen is necked and ruptured. For each of these forces, the cross-sectional dimensions can be measured and the stresses calculated, and then an approximate variability of the function $\sigma(\varepsilon)$ can be calculated. The values obtained in the strength tests and the quantities determined on their basis are depicted in Fig. 1. The plot $\sigma(\varepsilon)$ obtained from the testing machine is a conventional plot, the value of the force divided by a constant value of the cross-section is given on the vertical axis, whereas the elongation related to the initial length, that is to say, the relative strain (also called the conventional strain) is presented on the horizontal axis. Thus, as a matter of fact this diagram is a copy of the $\mathrm{F}(\Delta l)$ plot, in another system of coordinates. The quantities obtained on the basis of the strength tests are as follows:

1. limit of proportionality $\sigma_p = \sigma_{prop}$ and the strain corresponding to it $\varepsilon_p = \varepsilon_{prop}$ - and the Young's modulus E,
2. proof stress or physical yield point - R_{02} , R_e ($\sigma_0 = \sigma_{pl}$ and the strain corresponding to it $\varepsilon_0 = \varepsilon_{pl}$),
3. maximum force F_{max} - tensile strength R_m , real stress (σ_{rz}) corresponding to R_m, force corresponding to necking F_{kr} – maximum stress (σ_{max}) corresponding to rupture

Beside standard results given in typical reports, actual values of stresses corresponding to the tensile strength and the rupture force are given as well.

Table 1 Sample results of the tensile tests

No	Specimen dimensions b_o x h_o [mm]	Critical dimensions b_{min} x h_{min} [mm]	Extenso-meter base l_o [mm]	Proof stress $R_{0.2}$ [MPa]	Tensile strength R_m [MPa]	Real stresses corresponding to R_m σ_{rz} * [MPa]
1	59.65 x 1.86	40.08x1.46	50	243.9	297.3	357.2
2	66.30 x 1.86	43.40x1.35	50	204.6	317.4	394.1

No	Necked cross-section A_p[mm^2]	Elongation of the measured part $\Delta\, \boldsymbol{l}_{ex}$ [mm]	Maximum tensile force F_{max}[kN]	Force at which the test was stopped F_{kr} [kN]	Maximum tensile stress σ_{max} ** [MPa]	Unit elongation ε_{max} [%]
1	58.52	18.04	32.98	29.88	510.6	36.8
2	58.59	22.35	39.11	34.22	584.1	44.7

σ_{rz} * - real stresses corresponding to R_m,
σ_{max} ** - maximum stresses corresponding to rupture.

Note : the real stresses have been defined as a ratio of the maximum force to the area of the actual cross-section (according to formula 3), on the assumption that we have uniform tension until the maximum tensile force is achieved, e.g.:

$$\sigma_{rz} = \frac{F_{\max}}{b(\varepsilon) \cdot h(\varepsilon)} = \frac{F_{\max}}{b_0 h_0 \cdot (1 - \varepsilon_{kr} \cdot \nu_{pl})^2} = 357.2$$

and when this force is exceeded, we can observe a further development of plastic strains and an occurrence of necking, and the maximum stresses have been defined as a ratio of the rupture force to the necked cross-section area A_p:

$$\sigma_{\max} = \frac{F_{kr}}{A_p} = \frac{F_{\max}}{b_{\min} h_{\min}} = 510.6$$

3. Theoretical description of tension – modification of the Ramberg-Osgood curve

On the basis of physical and geometrical relations for plain stress, strains and stresses can be calculated if we characterise the material by the Ramberg-Osgood curve:

$$\varepsilon_{ij}^{pl} = \frac{3}{2}\alpha \cdot \varepsilon_o \left(\frac{\sigma_e}{\sigma_o}\right)^{n-1} \cdot \frac{S_{ij}}{\sigma_o} \tag{1}$$

The non-linear relationship $\sigma - \varepsilon$ is usually assumed in the form (assuming for simplicity that $p = 1/n$):

a)

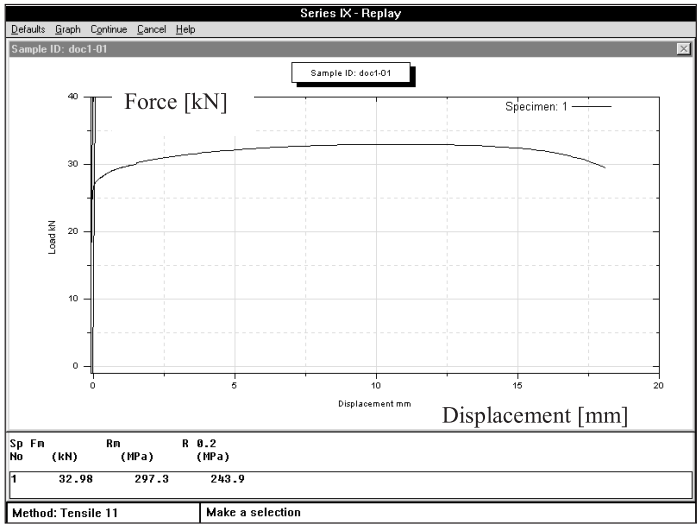

b)

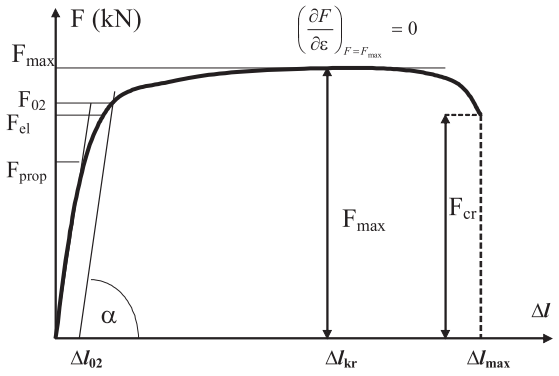

Figure 1 Tension diagrams F(Δl) - force-elongation: a) diagram obtained from the Instron testing machine, b) general diagram with characteristic quantities that enable a description of the material properties

$$\begin{aligned} \text{for } :\varepsilon \quad &\leq \quad \varepsilon_0 \quad \sigma = \left(\frac{\sigma_0}{\varepsilon_0}\right) \cdot \varepsilon \\ \text{for } :\varepsilon \quad &> \quad \varepsilon_0 \quad \varepsilon = \alpha \cdot \varepsilon_0 \cdot \left(\frac{\sigma}{\sigma_0}\right)^{\frac{1}{p}} \quad \Rightarrow \sigma = \tfrac{1}{\alpha}\sigma_0 \cdot \left(\frac{\varepsilon}{\varepsilon_0}\right)^{p} \end{aligned} \tag{2}$$

According to the author's point of view, an effect of transverse strains should be considered under large strains. To simplify the issue (for large plastic strains or elastic-plastic strains), one can assume that the dimensions of the rectangular cross-section ($b_0 \quad \times h_0$) change according to the following relationship:

$$b(\varepsilon_x) = b_0 \cdot (1 - \nu_{pl} \cdot \varepsilon_y), \quad h(\varepsilon_z) = h_0 \cdot (1 - \nu_{pl} \cdot \varepsilon_y), \quad \varepsilon_x = \varepsilon_z = -\nu_{pl} \cdot \varepsilon_y \tag{3}$$

and, for: $\varepsilon > \varepsilon_0$, the equivalent Poisson's ratio for elastic-plastic materials, according to [69], takes the form:

$$\nu_{pl} = \frac{1}{2} - \frac{1-2\cdot\nu_0}{2\cdot E_0}\cdot\frac{\sigma}{\varepsilon}, \quad \text{after the substitution of :} \qquad E_0 = \frac{\sigma_0}{\varepsilon_0} \quad \sigma = \sigma_0\cdot\left(\frac{\varepsilon}{\varepsilon_0}\right)^p \tag{4}$$

$$\nu_{pl} = \frac{1}{2} - \frac{1-2\cdot\nu_0}{2}\cdot\left(\frac{\varepsilon}{\varepsilon_0}\right)^{p-1} \quad \text{where: } \nu_0 \cong 0.3 \tag{5}$$

In individual phases of tension, we can determine approximately strains on the basis of tests, having the initial dimensions and the tension diagram in form (2).

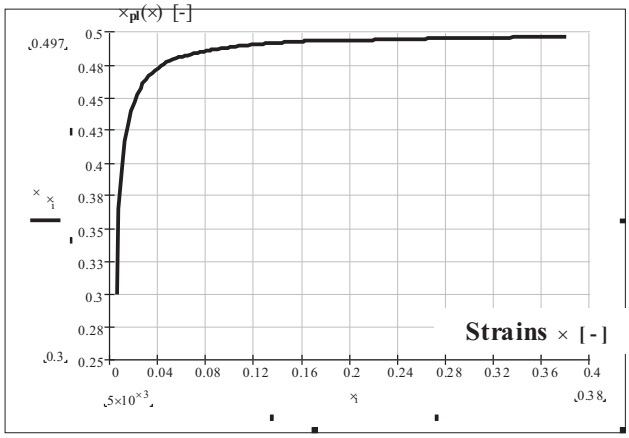

Figure 2 Changes in the Poisson's ratio $\nu_{pl}(\varepsilon\ )$ according to formula (5) as a function of strain $\nu(\varepsilon)$ for ν_0=0.3 and p=0.1

While analysing the tension process, we should consider the material strain hardening. Instead of the coefficient $(1/\alpha)$, we can assume the function $f(\varepsilon)$, which characterises the material strain hardening and necking. The value of the tensile force treated as a product of the stress and the cross-section can be calculated in approximation from the formula:

$$F_{rz} = f(\varepsilon)\cdot\sigma_o\cdot\left(\frac{\varepsilon}{\varepsilon_o}\right)^p\cdot b_0h_0\cdot(1-\nu_{pl}\cdot\varepsilon)^2 \tag{6}$$

The function $\sigma(\varepsilon)$ should also describe the material strain hardening and the effect of necking on the stresses under rupture; the function $f(\varepsilon)$ (proposed by the author) has been assumed as:

$$\sigma = f\,(\varepsilon)\cdot\sigma_0\cdot\left(\frac{\varepsilon}{\varepsilon_0}\right)^p \quad \text{where: } f(\varepsilon) = f_1(\varepsilon)\cdot f_2(\varepsilon) \tag{7}$$

The functions $f_1(\varepsilon)$ and $f_2(\varepsilon)$ have been selected in such a way that having employed the force-elongation or force-strain plot obtained from the testing machine, we can formulate the actual stress-strain $\sigma(\varepsilon)$ relationship. If the function $f_1(\varepsilon)$ characterises the linear strain hardening

$$f_1(\varepsilon) = 1 + A_1 \cdot \frac{\varepsilon}{\varepsilon_{kr}}$$

then, having the maximum value of the tensile force F_{max} and the strain ε_{kr} corresponding to it, obtained in tests, we can calculate the value of the exponent p and the strain hardening parameter A_1 from the equations:

$$\begin{gathered} \left(\frac{\partial F}{\partial \varepsilon}\right)_{F=F_{\max}} = 0, \quad (F)_{\varepsilon=\varepsilon_{kr}} = \\ = f(\varepsilon) \cdot \sigma_o \cdot \left(\frac{\varepsilon}{\varepsilon_o}\right)^p \cdot b_0 h_0 \cdot \left(1 - \left[\frac{1}{2} - \frac{1-2\cdot\nu_0}{2} \cdot \left(\frac{\varepsilon}{\varepsilon_0}\right)^{p-1}\right] \cdot \varepsilon\right)^2 = F_{\max} \end{gathered} \tag{8}$$

for instance, for the given values: b_0=59.65, h_0=1.86, L_0=200 mm, σ_0=240MPa, ε_0=0.001165, F_{max} 32.98kN, ε_{kr}=0.22.

Having solved system of equations 8, we obtain p =0.042 and the parameter A_1=0.254.

Simplifying the problem, that is to say, neglecting the influence of gripping in the machine jaws and considering the strains of the part under tension, when the yield point is exceeded, tension can be divided into two stages: uniform tension and an occurrence of necking. Uniform tension takes place until the maximum tensile force is achieved, and when it is exceeded, we can observe a further development of plastic strains and an occurrence of necking. Thus, the initial length can be divided theoretically into the part subjected to uniform tension (L_{01}) and the part that has been subjected to uniform tension and then to necking (L_{02}), as in Figs. 3 and 4.

The lengths L_{01} and L_{02} are calculated on the basis of the incompressibility condition, determined by strains and on the assumption that the total elongation of the specimen is a sum of elongations of both the parts (L_{01} and L_{02}), and the necked part (L_{02}) has been subjected to further strain by $\Delta\varepsilon$. These assumptions lead to the following system of equations:

$$\begin{gathered} L_{01} \cdot (1 + \varepsilon_{kr}) \cdot b_1 \cdot h_1 + L_{02} \cdot (1 + \varepsilon_{kr}) \cdot (1 + \Delta\varepsilon) \cdot b_2 \cdot h_2 = L_0 \cdot b_0 \cdot h_0 \\ L_{01} \cdot (1 + \varepsilon_{kr}) + L_{02} \cdot (1 + \varepsilon_{kr}) \cdot (1 + \Delta\varepsilon) = L_U \\ L_{01} + L_{02} = L_0 \end{gathered} \tag{9}$$

Having solved system of equations 9, we obtain the following values: L_{01}=84.76, L_{02}=115.25 (115.245), $\Delta\varepsilon$=0.347.

Taking into account the incompressibility condition defined by mean strains corresponding to the maximum tensile force and the rupture force, we calculate the length of the part subjected to uniform tension – L_{U1} and to necking – L_{U2} on the basis of the following formulae:

$$L_{U1} = L_{01} \cdot (1 + \varepsilon_{kr}), \quad L_{U2} = L_{02} \cdot (1 + \varepsilon_{kr}) \cdot (1 + \Delta\varepsilon) \tag{10}$$

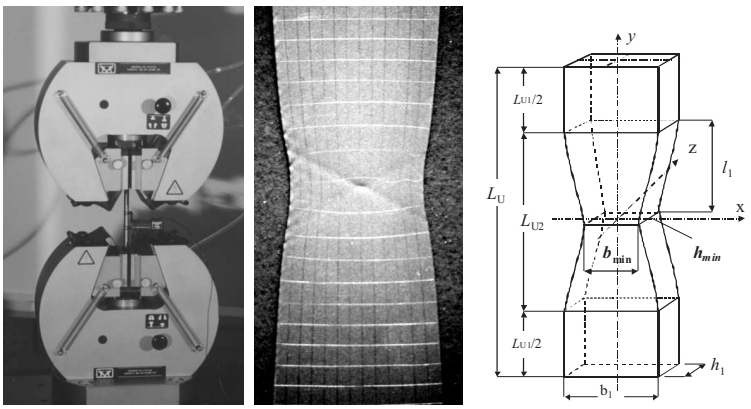

Figure 3 View of the specimens under test: a) in the grips of the testing machine with an extensometer, b) after the occurrence of necking, just before rupture, c) division into the part subject to tension (L_{01}) and the part that has been necked down (L_{02})

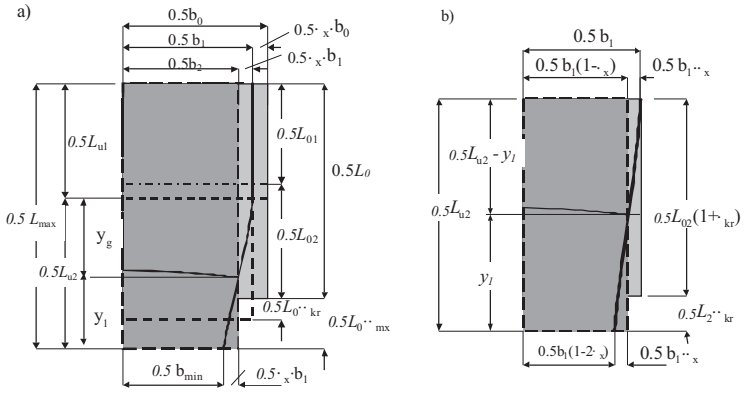

Figure 4 Subsequent phases of tension after exceeding the yield point: initial length L_0 divided into the part subjected to uniform tension $L_{01}$and the part that has been subjected to uniform tension and then to necking L_{02}

Changes in the cross-section of the specimen part subject to necking have a power character and vary according to relationship (4), (Fig. 5), and at the instant prior to rupture are equal to:

$$b_1 = b_0 \cdot (1 - \nu_{pl} \cdot \varepsilon_{kr}), \quad b_2 = b_1 \cdot (1 - \nu_{pl} \cdot \Delta\varepsilon), \quad b_{\min} = b_1 \cdot (1 - 2 \cdot \nu_{pl} \cdot \Delta\varepsilon), \tag{11}$$

analogously:
$h_1 = h_0 \cdot (1 - \nu_{pl} \cdot \varepsilon_{kr})$, $h_2 = h_1 \cdot (1 - \nu_{pl} \cdot \Delta\varepsilon)$, $h_{\min} = h_1 \cdot (1 - 2 \cdot \nu_{pl} \cdot \Delta\varepsilon)$,
where: $\nu_{pl} \cong 0.49$.

The length of the part subjected to necking – L_{U2} and the dimensions b_1, b_2 and b_{min} according to formulae (11) allow for a description of strains in bi-polar coordinates, and $l_1 = 0.5 \cdot L_{U2}$ has been assumed in the calculations.

The necking Z_{pl} with respect to the dimensions corresponding to the maximum tensile force is equal to:

$$Z_{pl} = \frac{b_1 \cdot h_1 - b_{\min} \cdot h_{\min}}{b_1 \cdot h_1} = 1 - (1 - 2 \cdot \nu_{pl} \cdot \Delta\varepsilon)^2$$

The function $f_2(\varepsilon)$ that describes necking has been calculated under the following assumptions made in the calculations: for the tensile force F_{max}, necking equals zero, and at the instant of rupture, we know the value of the rupture force F_Z and the dimensions of the cross-section. The function $f_2(\varepsilon)$ describing necking has been assumed as:

$$f_2(\varepsilon) = 1 - A_2 \cdot \left(\frac{\varepsilon}{\varepsilon_m}\right)^{w/p} \tag{12}$$

The constant A_2 and the exponent w have been calculated on the assumption that necking occurs when the maximum tensile force is exceeded and the changes in the cross-section have a power character, and on the assumption that $\nu_{pl} \cong 0.495$. Then the dimensions of the cross-section change according to relationship (11), (Fig. 5) and are equal to (b_{min}, h_{min}) at the instant of rupture, and thus we obtain the equations:

$$\begin{gathered} f_2(\varepsilon_{kr}) = 1 \quad f_2(\varepsilon_{\max}) = 1 - (1 - 2 \cdot \nu_{pl} \cdot \Delta\varepsilon)^2 \\ f_1(\varepsilon) \cdot \sigma_o \cdot \left(\frac{\varepsilon}{\varepsilon_o}\right)^p \cdot b_0 h_0 \cdot \left[1 - A_2 \cdot \left(\frac{\varepsilon}{\varepsilon_m}\right)^{\frac{w_1}{p}}\right] \cdot (1 - \nu_{pl} \cdot \varepsilon)^2 = F_{Zr} \end{gathered} \tag{13}$$

For the previously given values of A_1, p and for the rupture force $F_{zr} = 3.1$ kN, $\varepsilon = 0.347$, ($\varepsilon = \Delta\varepsilon$), we obtain A_2=0.285, w=0.862 and the value of strains in the necked part that corresponds to rupture is $\varepsilon_m = 0.407$.

Having calculated the strain hardening and necking parameters, we obtain the plots of the tensile force $F_{rz}(\varepsilon)$, or $F(\Delta l)$, as a function of elongation (these plots are shown in Fig. 5):

$$F_{rz} = f_1(\varepsilon) \cdot f_2(\varepsilon) \cdot \sigma_o \cdot \left(\frac{\varepsilon}{\varepsilon_o}\right)^p \cdot b_0 h_0 \cdot \left(1 - \left[\frac{1}{2} - \frac{1 - 2 \cdot \nu_0}{2} \cdot \left(\frac{\varepsilon}{\varepsilon_0}\right)^{p-1}\right] \cdot \varepsilon\right)^2 \tag{14}$$

and of the stresses $\sigma(\varepsilon)$ as a function of conventional strains for $\varepsilon_0 \leq \varepsilon \leq \varepsilon_{max}$:

$$\sigma_{rz} = \frac{F_{rz}}{b(\varepsilon) \cdot h(\varepsilon)}, \quad \text{or approximately: } \sigma(\varepsilon) = f_1(\varepsilon) \cdot \sigma_o \cdot \left(\frac{\varepsilon}{\varepsilon_o}\right)^p \tag{15}$$

3.1. *Conventional and logarithmic strain*

Other methods of the description of the relationship $F(\varepsilon)$ have been presented in [4, 5, 17, 18,]. Starting from the logarithmic strains $\overrightarrow{\varepsilon}$ proposed by Ludwik [7],

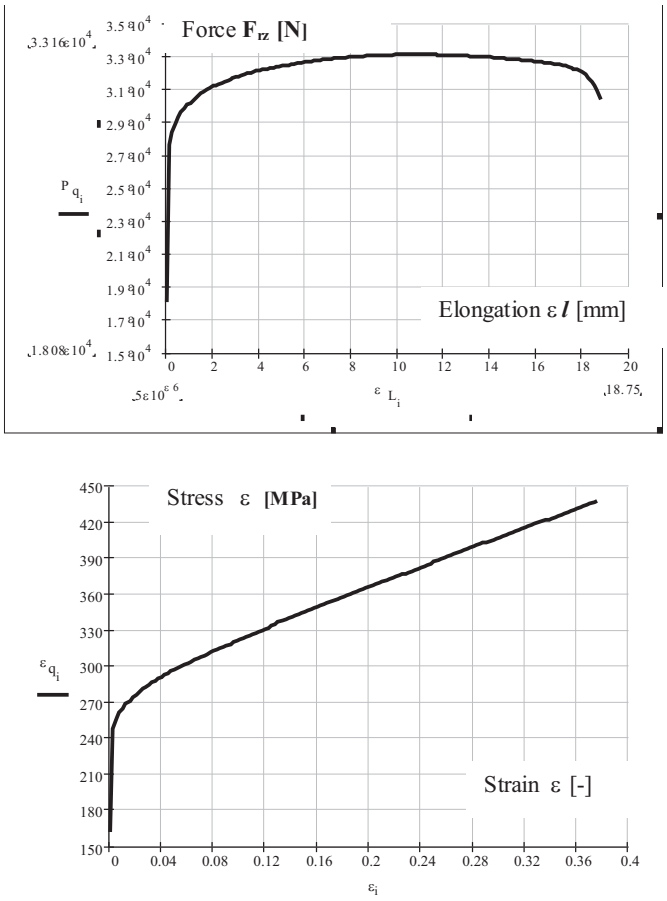

Figure 5 Tension diagrams F(Δl) and $\sigma(\varepsilon)$ obtained from the calculations according to formulae (14) and (15), taking into account strain hardening and necking

the conventional strain ε is related to the logarithmic one $\overrightarrow{\varepsilon}$ by the following relationship: $\overrightarrow{\varepsilon} = \ln(1+\varepsilon)$. An elementary increment of the conventional strain dε expresses a change in the length with respect to the initial length l_0, whereas an increment of the logarithmic strain $d\overrightarrow{\varepsilon}$ expresses a change of the length with respect to the instantaneous length l. These strains are written as follows:

$$d\varepsilon = \frac{dl}{l_0} \quad \Rightarrow \quad \varepsilon = \frac{l-l_0}{l_0}, d\overrightarrow{\varepsilon} = \frac{dl}{l} \Rightarrow \overrightarrow{\varepsilon} = \ln\frac{l}{l_0} \tag{16}$$

where: $l = l_0(1+\varepsilon)$, and thus we obtain: $\overrightarrow{\varepsilon} = \ln(1+\varepsilon)$

Taking into account the above-mentioned assumptions, we can calculate the value of the tensile force from the formula:

$$F = \sigma(\varepsilon) \cdot A(\varepsilon) \tag{17}$$

where the stresses $\sigma(\varepsilon)$ and the cross-section$A(\varepsilon)$are functions of strains. Starting

with the condition of instability in tension, that is to say, for $\mathrm{F} = \mathrm{F}_{max}$, $\partial \mathrm{F}/\partial\varepsilon_1 = 0$ (on assumption that ε_1 corresponds to the tension direction, and ε_2 and ε_3 are main strains perpendicular to ε_1), the following has been obtained:

$$\frac{dF}{d\varepsilon_1} = \frac{d\sigma}{d\varepsilon_1} \cdot A + \sigma \cdot \frac{dA}{d\varepsilon_1} = 0, \quad \text{where: } A = A_0 \cdot (1+\varepsilon_2) \cdot (1+\varepsilon_3) = A_0 \cdot e^{\overrightarrow{\varepsilon_2}} \cdot e^{\overrightarrow{\varepsilon_3}} \quad (18)$$

Having taken into account the incompressibility condition that is defined by the logarithmic dilatational strain:

$$\Delta\overrightarrow{V} = \ln(1+\Delta V) = \overrightarrow{\varepsilon_1} + \overrightarrow{\varepsilon_2} + \overrightarrow{\varepsilon_3} \quad \Delta\overrightarrow{V} = 0 \quad \overrightarrow{\varepsilon_1} + \overrightarrow{\varepsilon_2} + \overrightarrow{\varepsilon_3} = 0 \Rightarrow \overrightarrow{\varepsilon_2} + \overrightarrow{\varepsilon_3} = -\overrightarrow{\varepsilon_1}$$

and $A_1 = A_0 \cdot e^{-\overrightarrow{\varepsilon_1}}$, we obtain: $\frac{dA}{d\overrightarrow{\varepsilon_1}} = -A_0 \cdot e^{-\overrightarrow{\varepsilon_1}} = -A$

Having substituted the above-mentioned equation into (18) and having divided it by A, we get the condition of instability in tension as follows:

$$\frac{d\sigma}{d\varepsilon_1} = \sigma_1 \quad (19)$$

The conventional dilatational strain (ΔV) is equal to:

$$\Delta V = (1+\varepsilon_1)(1+\varepsilon_2)(1+\varepsilon_3) - 1 = J_1 + J_2 + J_3$$

J_1, J_2, J_3 – are invariants of the strain tensor. Under large strains, the assumption that the conventional dilatational strain can be expressed only by the first invariant of the strain tensor, i.e. $\Delta V \cong \varepsilon_1 + \varepsilon_2 + \varepsilon_3 = \mathrm{J}_1$, is a kind of approximation, and thus does not present precisely the dilatational strain. Bearing in mind the above-mentioned assumptions, the value of the tensile force on the basis of (17) is equal to:

$$F = \sigma(\varepsilon) \cdot A_0 \cdot e^{-\overrightarrow{\varepsilon_1}} or, if e^{\overrightarrow{\varepsilon_1}} = 1 + \varepsilon_1 and \varepsilon_1 = e^{\overrightarrow{\varepsilon_1}} - 1, then F = \sigma(\varepsilon) \cdot \frac{A_0}{1+\varepsilon_1} \quad (20)$$

Assuming in the calculations the relationship $\sigma(\varepsilon)$ according to formula (3) for the rectangular cross-section $\mathrm{A}_0 = \mathrm{b}_0 \cdot h_0$, we obtain the value of the force as a function of strains:

$$F = \sigma_o \cdot \left(\frac{\varepsilon}{\varepsilon_o}\right)^p \cdot \frac{b_0 h_0}{1+\varepsilon} \quad (21)$$

Having introduced the function g(ε), we obtain:

$$F_n = g(\varepsilon) \cdot \sigma_o \cdot \left(\frac{\varepsilon}{\varepsilon_o}\right)^p \cdot \frac{b_0 h_0}{1+\varepsilon} \quad (22)$$

The function$g(\varepsilon) = g_1(\varepsilon) \cdot g_2(\varepsilon)$, which characterises strain hardening and necking, has been assumed in an analogous form according to formulae (7) and (12):

$$g_1(\varepsilon) = 1 + B_1 \cdot \frac{\varepsilon}{\varepsilon_{kr}}, \quad g_2(\varepsilon) = 1 - B_2 \cdot \left(\frac{\varepsilon}{\varepsilon_m}\right)^{u/p}$$

and the parameters B_1 and p have been calculated as previously for $\varepsilon = \varepsilon_{kr}$, $F_n = F_{max}$ and $(\partial F_n/\partial\varepsilon) = 0$ and for the same given values of σ_0, ε_0, ν_0, $\varepsilon_{zn} \cong \varepsilon_{max}$ and the initial dimensions b_0 and $h_0$according to the formulae:

$$\left(1 + B_1 \frac{\varepsilon}{\varepsilon_{kr}}\right) \cdot \sigma_o \cdot \left(\frac{\varepsilon}{\varepsilon_o}\right)^p \cdot \frac{b_0 h_0}{1+\varepsilon} = F_{\max}$$

$$\frac{B_1}{\varepsilon_{kr}} + \left(1 + B_1 \frac{\varepsilon}{\varepsilon_{kr}}\right) \cdot \frac{p}{\varepsilon} - \left(1 + B_1 \frac{\varepsilon}{\varepsilon_{kr}}\right) \cdot \frac{1}{1+\varepsilon} = 0$$

$\Rightarrow$p = 0.053, B_1= 0.146. The parameters B_2, u and $\varepsilon_m$have been calculated employing the equations analogous to (13):

$$\begin{gathered} g_2(\varepsilon_{kr}) = 1 \quad g_2(\varepsilon_{\max}) = 1 - (1 - 2 \cdot \nu_{pl} \cdot \Delta\varepsilon)^2 \\ \left(1 + B_1 \frac{\varepsilon}{\varepsilon_{kr}}\right) \cdot \left[1 - B_2 \cdot \left(\frac{\varepsilon}{\varepsilon_m}\right)^{\frac{u}{p}}\right] \cdot \sigma_o \cdot \left(\frac{\varepsilon}{\varepsilon_o}\right)^p \cdot \frac{b_0 h_0}{1+\varepsilon} = F_{zr} \end{gathered} \tag{23}$$

and thus we obtain: B_2= 0.606, u = 0.147, ε_{zn} = 0338, ε_m = 0.43

The values of actual stresses have been obtained by dividing the tensile force $F(\varepsilon)$ by the cross-section, and for $\varepsilon_0 \leq \varepsilon \leq \varepsilon_{max}$, they have been calculated according to the following formulae:

$$\begin{gathered} F_n = \left(1 + B_1 \frac{\varepsilon}{\varepsilon_{kr}}\right) \cdot \left[1 - B_2 \cdot \left(\frac{\varepsilon}{\varepsilon_m}\right)^{\frac{u}{p}}\right] \cdot \sigma_o \cdot \left(\frac{\varepsilon}{\varepsilon_o}\right)^p \cdot \frac{b_0 h_0}{1+\varepsilon}, \\ \sigma(\varepsilon) = g_1(\varepsilon) \cdot \sigma_o \cdot \left(\frac{\varepsilon}{\varepsilon_o}\right)^p \end{gathered} \tag{24}$$

4. Theoretical description of strains in bi-polar coordinates - generalisation of the Bridgman solution

The analysis of the state of strain and stress in necking has been described in [1, 4] and al. However, the state of stress has been generally analysed in necking and a description of strains has been presented in cylindrical coordinates. In the present study, the state of strain and stress has been described in the whole specimen (neglecting the gripped parts only) with bi-polar coordinates (these coordinates have been described, among others, in books [3], [11]). The strain distributions corresponding to the phase prior to the specimen fracture in bi-polar coordinates are shown in Fig. 7. The lines showing main strains obtained experimentally can be described approximately in bi-polar coordinates by dividing the specimen into two basic elements: necking in the place of rupture and the "gripped" part that is subject to smaller plastic strains (Fig. 7). The location of necking has been described by means of the variables: ζ, α, β.

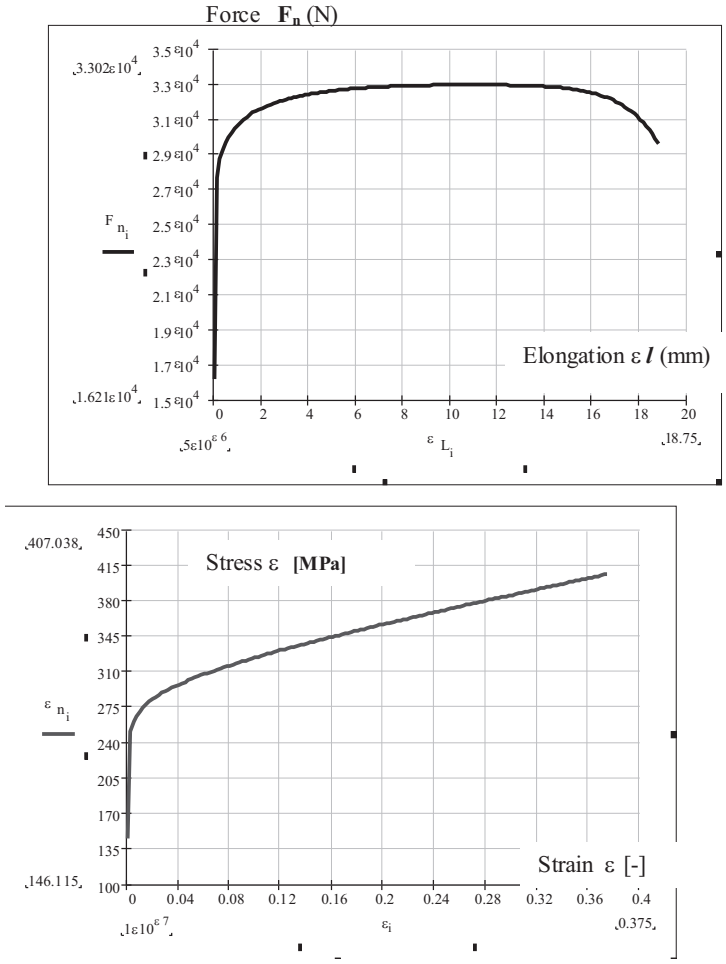

Figure 6 Tension diagrams: a) $F_n(\Delta l)$ and b) - $\sigma(\varepsilon)$ obtained on the basis of the calculations according to formulae (23) and (24), having taken into account strain hardening and necking

$$\begin{gathered}
\zeta = \alpha + i \cdot \beta \quad \text{and} \zeta = \ln \frac{a+z}{a-z} \quad \text{where: } z = x + i \cdot y \\
x = \frac{a \cdot \sinh(\alpha)}{\cosh(\alpha)+\cos(\beta)} y = \cdot \frac{a \cdot \sin(\beta)}{\cosh(\alpha)+\cos(\beta)} \quad \alpha = \ln \frac{\sqrt{(x+a)^2+y^2}}{\sqrt{(x-a)^2+y^2}} \\
\beta = arctg\frac{y}{a+x} - arctg\frac{y}{a-x} \rho_1 = \frac{a_1}{|sh\alpha_o|} \quad R_1 = \frac{a_1}{|\sin\beta_o|} \\
d_1 = a_1 \cdot |ctgh\alpha_o| \quad r_1 = a_1 \cdot \left|tgh\frac{\alpha_o}{2}\right|
\end{gathered} \tag{25}$$

Strains in the part subject to smaller plastic strains have been also presented in the bi-polar coordinates η, R_2 and ξ, ρ_2. For the "gripped" part, strains have been described through a transformation of the coordinate system (rotation by 90 $^\circ$ and

translation by L) with an exchange of variables. The lines α=const transform into the lines ξ, the lines β=const transform into the lines ηog$\zeta_2 = \xi + i \cdot \eta$).

$$x_2 = \frac{a_2 \cdot \sin(\eta)}{\cosh(\xi)+\cos(\eta)}, \quad y_2 = l_1 - \frac{a_2 \cdot \sinh(\xi)}{\cosh(\xi)+\cos(\eta)} \quad l_1 = \frac{a_1 \cdot \sin\beta}{\cosh\alpha+\cos\beta} + \frac{a_2 \cdot \sinh\xi}{\cosh\xi+\cos\eta},$$

$$\rho_2 = \frac{a_2}{|sh\xi|} \quad , \quad R_2 = \frac{a_2}{|\sin\eta|} \quad , \quad b_0 = 2 \cdot a_2 \cdot \left|tg\frac{\eta_o}{2}\right| \tag{26}$$

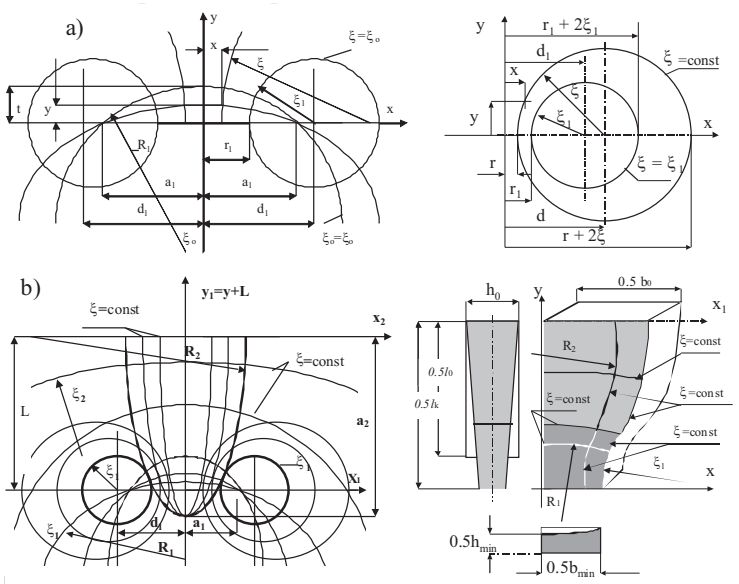

Figure 7 Bi-polar coordinates assumed in the calculations: a) main strain line curvatures, b) division into two basic elements: necking and the rupture point, and the "gripped" part

The solution to the problem in cylindrical coordinates is presented in, for instance, [1, 4]. In these references, an approximate integration of the equations of equilibrium for specimens with the circular cross-section has been performed. In the case of flat specimens, an analogous method can be used. The description of strains in bi-polar coordinates enables a division into two basic elements: necking (point of rupture) and a part that is subject to smaller plastic strains.

4.1. *Calculations of strains*

The strains corresponding to necking, obtained on the basis of the experimental data, can be described in bi-polar coordinates. The specimen length subject to necking – L_{U2}= $2 \cdot l_1$,the radii of main curvatures ρ_2 and R_2, the specimen width b_1 are equal to, respectively:

$$l_1 = \frac{a_1 \cdot \sin\beta}{\cosh\alpha+\cos\beta} + \frac{a_2 \cdot \sinh\xi}{\cosh\xi+\cos\eta} \quad \rho_2 = \frac{a_2}{|sh\xi|} \quad R_2 = \frac{a_2}{|\sin\eta|} \quad b_1 = a_2 \cdot \left|tg\frac{\eta_o}{2}\right| \tag{27}$$

In the upper part, the variables ξ, η have to satisfy the conditions $0 \leq \eta \leq \eta_0$, - $\xi_0 \leq \xi \leq 0$.

On the other hand, it has been assumed that the dimensions of the cross-section vary according to relationship (11), where: $\Delta\varepsilon = \varepsilon_{\max} - \varepsilon_{kr}$ and the length l_1 is equal to half the length of L_{U2}, hence $l_1 = 0.5 \cdot L_{U2}$,

$$L_{U2} = L_{01} \cdot (1 + \varepsilon_{kr}) \cdot (1 + \Delta\varepsilon)$$

Taking into account relationships (23) and (24) and the conditions of continuity along the joint of the lower and upper part, we obtain a system of equations that allows us to describe strains in bi-polar coordinates:

$$\begin{gathered} b_0 \cdot (1 - \nu_{pl} \cdot \varepsilon_{kr}) = 2 \cdot a_2 \cdot \left| tg\tfrac{\eta_o}{2} \right|, \\ b_0 \cdot (1 - \nu_{pl} \cdot \varepsilon_{kr}) \cdot (1 - 2 \cdot \nu_{pl}\Delta\varepsilon) = 2 \cdot a_1 \cdot \left| tgh\tfrac{\alpha_o}{2} \right|, \\ l_1 = \tfrac{a_1 \cdot \sin(\beta_0)}{1+\cos(\beta_0)} + \tfrac{a_2 \cdot \sinh(\xi_0)}{\cosh(\xi_0)+1}, \quad \tfrac{a_1 \cdot \sinh(\alpha_0)}{\cosh(\alpha_0)+\cos(\beta_0)} = \tfrac{a_2 \cdot \sin(\eta_0)}{\cosh(\xi_0)+\cos(\eta_0)}, \\ \tfrac{a_1}{|\sin\beta_o|} = \tfrac{a_2}{|sh\xi_0|}, \quad l_1 = \tfrac{a_1 \cdot \sin(\beta_0)}{\cosh(\alpha_0)+\cos(\beta_0)} + \tfrac{a_2 \cdot \sinh(\xi_0)}{\cosh(\xi_0)+\cos(\eta_0)} \end{gathered} \tag{28}$$

Additionally, it is known that: $\sin^2\beta_0 + \cos^2\beta_0 = 1$, $\cosh^2\alpha_0 - \sinh^2\alpha_0 = 1$, $\sin^2\eta_0 + \cos^2\eta_0 = 1$, $\cosh^2\xi_0 - \sinh^2\xi_0 = 1$.

The data for calculations are assumed on the basis of the experimental investigations.

The initial dimensions are as follows: $b_0 = 60.0$mm, $h_0 = 1.86$mm, $l_1 = 93.147$ mm, the coefficient of deformation ν_{pl}, corresponding to the Poisson's ratio, has been calculated according to (5), the values of strains corresponding to the maximum tensile force ε_{kr} and the force corresponding to rupture ε_{max} are equal to $\varepsilon_{kr} = 0.2$, $\varepsilon_{max} = 0.375$ ($\varepsilon_{max} = 0.44$), respectively.

The dimensions of the specimen after it has been subjected to strain and necking are as follows: $b_1 = 54.06$mm, $b_2 = 47.64$ mm, $b_{min} = 40.08$mm $\Rightarrow b_1 = b_0(1 - 2\nu_{pl}\Delta\varepsilon_k)$

Having solved system of equations (28), we obtain the parameters that describe changes in the specimen dimensions corresponding to necking in bi-polar coordinates:

$a_1 = 112.18$mm, $\rho_1 = 304.09$mm, $\alpha_0 = 0.361$, $\beta_0 = 0.795$, $R_1 = 157.14$ mm and $a_2 = 128.76$ mm, $\rho_2 = 157.1$ mm, $\eta_0 = 0.414$, $R_2 = 280.8$mm, $\xi_0 = -0.748$.

Employing the equations of equilibrium for the Cartesian system of coordinates (x, y), assumed for the whole specimen, the state of strain in the phase prior to rupture can be described:

$$\frac{\partial\sigma_x}{\partial x} + \frac{\partial\tau_{xy}}{\partial y} = 0, \quad \frac{\partial\tau_{xy}}{\partial x} + \frac{\partial\sigma_y}{\partial y} = 0$$

Assuming that the relationships between main strain lines in the phase of plastic yield can be described in approximation by the proportions:

$$\frac{r_1}{x} = \frac{x + 2\rho}{r_1 + 2\rho_1} \quad \Rightarrow \quad \frac{1}{\rho} = \frac{2x}{r_1^2 + 2\rho_1 r_1 - x^2} \tag{29}$$

Next, assuming that:

$$\tau_{xy} = \frac{\sigma_y - \sigma_x}{2} \sin 2\varphi \equiv \sigma_{int}\varphi \quad \text{for}\varphi \quad \to 0 \sin 2\varphi \cong 2\varphi, \quad \varphi \cong \frac{y}{\rho} \tag{30}$$

for y = 0 $\sigma_y - \sigma_x = \sigma_{int}$ on the basis of the first equation of equilibrium:
$\frac{\partial \tau_{xy}}{\partial y} = \sigma_{int}\frac{\partial \varphi}{\partial y}$, $\frac{\partial \sigma_x}{\partial x} = -\sigma_{int} \cdot \frac{2x}{r_1^2 + 2\rho_1 r_1 - x^2} \Rightarrow \quad \sigma_x = \sigma_{int} \cdot \ln\left(r_1^2 + 2\rho_1 r_1 - x^2\right) + C$

The constant C can be calculated from the condition for x = r_1 σ_x= 0 , then for y⇒0

$$\sigma_x = \sigma_{int} \cdot \ln \frac{r_1^2 + 2\rho_1 r_1 - x^2}{2\rho_1 r_1} \quad \sigma_y = \sigma_{int} \cdot \left(1 + \ln \frac{r_1^2 + 2\rho_1 r_1 - x^2}{2\rho_1 r_1}\right) \tag{31}$$

whereas, for y≠0, one should check if the second equation of equilibrium and boundary conditions are fulfilled.

Assuming that $\tau_{xy} \equiv \sigma_{int} \cdot \varphi = \sigma_{int} \cdot \frac{2xy}{r_1^2 + 2\rho_1 r_1 - x^2}$ on the basis of the second equation of equilibrium, we obtain:

$$\sigma_y = -\sigma_{int} \cdot \left(\frac{y^2}{r_1^2 + 2\rho_1 r_1 - x^2} + \frac{2x^2 y^2}{(r_1^2 + 2\rho_1 r_1 - x^2)^2}\right) + C_2$$

hence, the constant C_2 can be calculated if we know the stress σ_y for y=0 according to formula (31), and thus:

$$\sigma_y = \sigma_{int} \cdot \left(1 + \ln \frac{r_1^2 + 2\rho_1 r_1 - x^2}{2\rho_1 r_1} - \frac{y^2\left(r_1^2 + 2\rho_1 r_1 + x^2\right)}{(r_1^2 + 2\rho_1 r_1 - x^2)^2}\right) \tag{32}$$

The above-mentioned solution describes the components of stresses in Cartesian coordinates. However, taking into account changes in curvatures of main strains, it is easier to describe the components of stresses in the part subject to necking in curvilinear coordinates.

4.2. *Analysis of stresses in bi-polar coordinates*

On the basis of physical and geometrical relations for plane stress for flat specimens, strains and stresses can be calculated on the basis of the Lamé equations, then the following equations hold in necking:

$$\frac{\partial \sigma_\beta}{\partial s_\alpha} + \frac{\sigma_\beta - \sigma_\alpha}{R_1} = 0, \quad \frac{\partial \sigma_\alpha}{\partial s_\beta} + \frac{\sigma_\beta - \sigma_\alpha}{\rho_1} = 0 \tag{33}$$

Assuming that $\sigma_{int} = \sigma_\beta - \sigma_\alpha$, we obtain:

$$\begin{gathered} \sigma_\alpha = \sigma_{int} \cdot \ln \frac{\cosh \alpha_o + \cos \beta}{\cosh \alpha + \cos \beta} \quad \sigma_\beta = \sigma_{int} \cdot \left[1 + \ln \frac{(\cosh \alpha_o + 1) \cdot (\cosh \alpha + \cos \beta)}{(\cosh \alpha + 1)^2}\right] \\ \sigma_z = 0 \quad \varepsilon_z = -\left(\frac{\sigma_{int}}{\sigma_o}\right)^{n-1} \cdot \frac{\varepsilon_o}{2\sigma_o}\left(\sigma_\alpha + \sigma_\beta\right) \end{gathered} \tag{34}$$

The specimen thickness h(α,β) can be calculated in approximation according to:

$$h(\alpha, \beta) = h_0 \cdot (1 + \varepsilon_z) = h_0 \cdot \left[1 - \left(\frac{\sigma_{int}}{\sigma_o}\right)^{n-1} \cdot \frac{\varepsilon_o}{2\sigma_o}\left(\sigma_\alpha + \sigma_\beta\right)\right] \tag{35}$$

Under the assumption of plane stress on the specimen surface, the intensities of stresses and strains are equal to, respectively:

$$\sigma_{int} = \sqrt{\sigma_\alpha^2 - \sigma_\alpha \sigma_\beta + \sigma_\beta^2}, \quad \varepsilon_{int} = \varepsilon_0 \cdot \left(\frac{\sigma_{int}}{\sigma_0}\right)^n \tag{36}$$

where σ_{int} is the stress intensity according to the Huber – Mises hypothesis.

On the basis of the boundary conditions along the line that connects the upper and lower part: for $\beta = \pi/2$ and ξ = -$\pi/2$, $\sigma_\beta = \sigma_\xi$ and $\sigma_\alpha = \sigma_\eta$ for $\eta = 0.492$, $\sigma_\eta = 0$, for $y = L$ $\sigma_y = \sigma_o$, and then we obtain the stress components.

In the "gripped" part, the Lamé equations have the form:

$$\begin{gathered} \frac{\partial \sigma_\xi}{\partial s_\eta} + \frac{\sigma_\xi - \sigma_\eta}{\rho_2} = 0 \quad \frac{\partial \sigma_\eta}{\partial s_\xi} + \frac{\sigma_\xi - \sigma_\eta}{R_2} = 0 \\ \sigma_{\eta i} = -\sigma_{0i} \cdot \ln \frac{\cosh \xi_i + \cos \eta_0}{\cosh \xi_i + \cos \eta_i}, \quad \sigma_{\xi i} = \sigma_{oi} \cdot \left[1 - \ln \frac{(1+\cos \eta_0)\cdot(\cosh \xi_i + \cos \eta_i)}{(1+\cos \eta_i)^2}\right] \end{gathered} \tag{37}$$

where σ_{0i} is the stress acting along the line connecting the upper and lower part, calculated on the basis of the conditions of continuity along the line $\beta_o = \xi_o$= const.

$$\sigma_{0i} = \sigma_{int} \cdot \left[1 + \ln \frac{(\cosh \alpha_0 + 1)\cdot(\cosh \alpha_i + \cos \beta_0)}{(\cosh \alpha_i + 1)^2}\right] \cdot \left[\left[1 - \ln \frac{(1+\cos \eta_0)\cdot(\cosh \xi_i + \cos \eta_0)}{(1+\cos \eta_i)^2}\right]^{-1}\right]$$

A mean value of the stress intensity σ_{int} can be calculated if the dimensions of the specimen in its cross-section subject to necking are known. Having divided the force causing necking by the cross-section corresponding to it for β=0, we obtain the integral equation, on the basis of which we calculate σ_{int}:

$$\sigma_{int} = \frac{F_{zr}}{2 \cdot \int\limits_0^{\alpha_0} h(\alpha, \beta) \cos \varphi \cdot ds_\beta} \tag{38}$$

where F_{zr} is calculated from formula (14), and h(α,β) – from formula (35). An example of calculations of the stress intensity (σ_{int}) is shown in Fig. 13.

Example of calculations

$$\sigma_{\mathrm{int}_i} = \frac{\left[1+0.146\left(\frac{\varepsilon_i}{\varepsilon_{kr}}\right)\right]\left[1-B_2\left(\frac{\varepsilon_i}{\varepsilon_m}\right)^{\frac{u}{p}}\right]\sigma_0\left(\frac{\varepsilon_i}{\varepsilon_0}\right)^p \frac{b_0 h_0}{1+\varepsilon_i}}{2\int_0^{0.3481} h_0\left[1-\frac{1}{2}\left(\frac{\sigma_{n_i}}{\sigma_0}\right)^n \varepsilon_0\left[1+\ln\left[\frac{(\cosh(\alpha_0)+1)(\cosh(\alpha_0)+\cos(\beta_0))}{(\cosh(\alpha)+1)^2}\right]\right]\right]\left(\frac{a_1}{\cosh(\alpha)+\cos(\beta_0)}\right)d\alpha}$$

$$\sigma_n(\varepsilon) = g_1(\varepsilon) \cdot \sigma_o \cdot \left(\frac{\varepsilon}{\varepsilon_o}\right)^p, \quad \sigma_{\log}(\varepsilon) = \sigma_n(\varepsilon) \cdot (1 + \varepsilon) \tag{39}$$

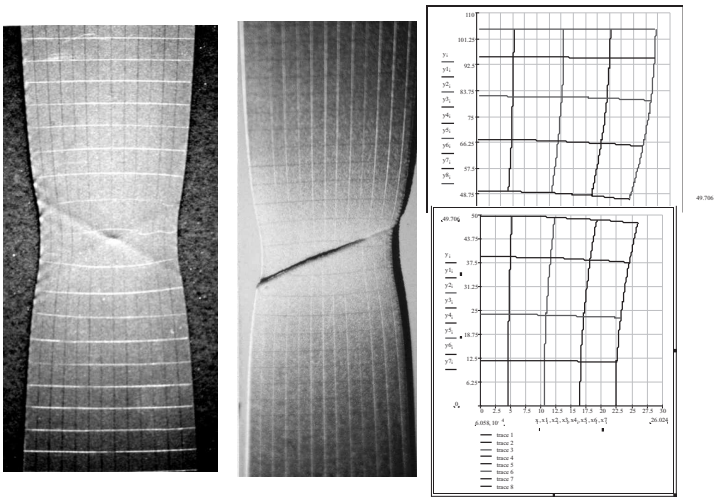

Figure 8 Distribution of strains in the failure phase for St3s and St4s steel and the strain lines in bi-polar coordinates, with a division into two basic elements: the point of rupture and the gripped part

5. Description of the displacement measurement method and results of tests and calculations

Displacements of the specimen surface in the point of an occurrence of necking and fracture just before failure were determined by means of the moiré–fringe technique. Owing to the simplicity of this method and relatively large strains, a shadow method was employed. [10,13]. The measurement principle has been shown in Fig. 10. Moiré half-tone screens were located parallel to the specimen surface, then the specimens were illuminated at the angle

$\varphi \quad = 30^\circ \div 40^\circ$, and the moiré–fringe patterns corresponding to perpendicular displacements that characterise changes in thickness and sliding lines were photographed.

Next, the results of tests and calculations were compared for the given values: e=1/13mm, $\varphi_1 \quad = \quad 40^\circ$, $\quad \varphi_2 = 34^\circ$, w $\cong$ 0.051mm.

The difference in height corresponding to the distance S between the neighbouring moiré-fringe patterns was calculated according to the formula:

$$w = \frac{e}{tg\varphi_1 + tg\varphi_2} \tag{40}$$

where:
e – mesh pitch (distance between mesh lines per 1 mm)
w – difference in height corresponding to the length S between the subsequent moiré-fringe patterns
φ_1 – angle of incidence of the parallel light beam
φ_2 – camera inclination angle
w = 8· 0.051 = 0.408 mm, 2w = 0.816, h_s= 0.54 ÷0.66 mm, h_{min}= 1.356 ÷1.476 mm (1.4 mm)

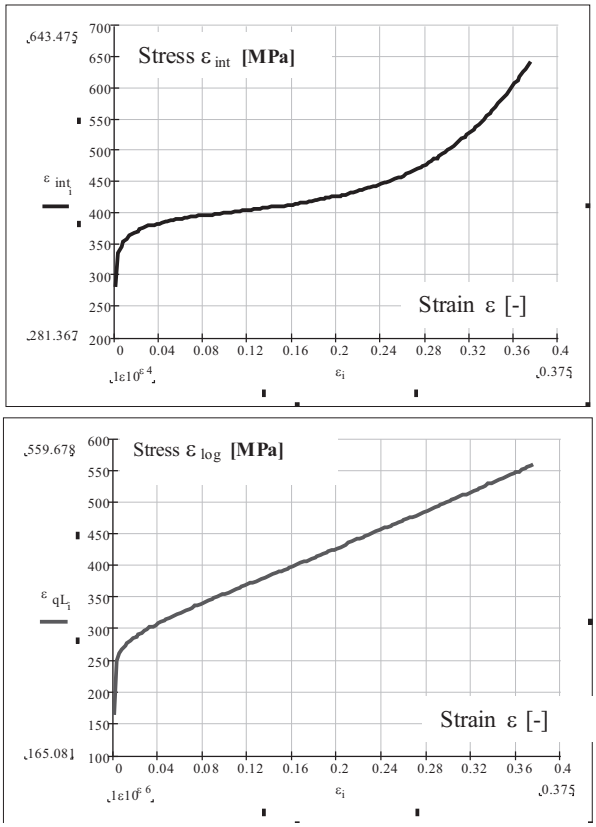

Figure 9 Tension diagrams $\sigma(\varepsilon)$ obtained according to formula (41), after taking into account strain hardening and necking, and according to formula (42) as a function of logarithmic strains according to formula (16)

5.1. *Results of analytical calculations of stresses and strains in the phase prior to rupture*

The analysis of strains and stresses made by means of analytical and numerical methods was based on tensile tests in the phase of failure. The results of analytical numerical calculations obtained with the 'MATHCAD 2001" software package and the FEM code (ANSYS 6.1 and 9.0) are presented below. The distributions of stresses σ_β and σ_α calculated on the basis of equations (34) and the intensities of stresses and strains in the necking region (as a function of the coordinates α and β) according to (36) are depicted in Figs. 13 ÷ 18.

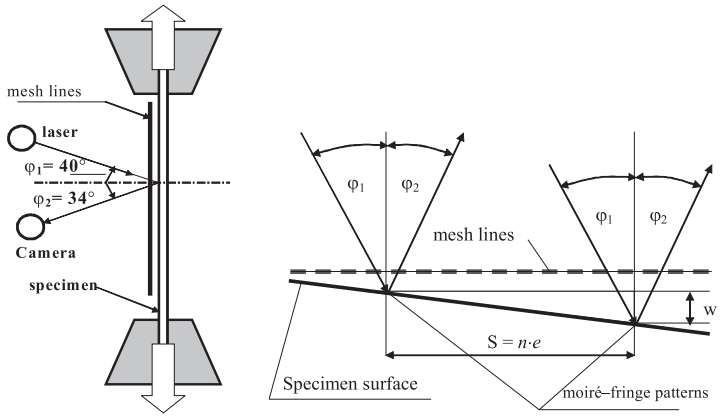

Figure 10 Displacement measurement principle on the specimen surface

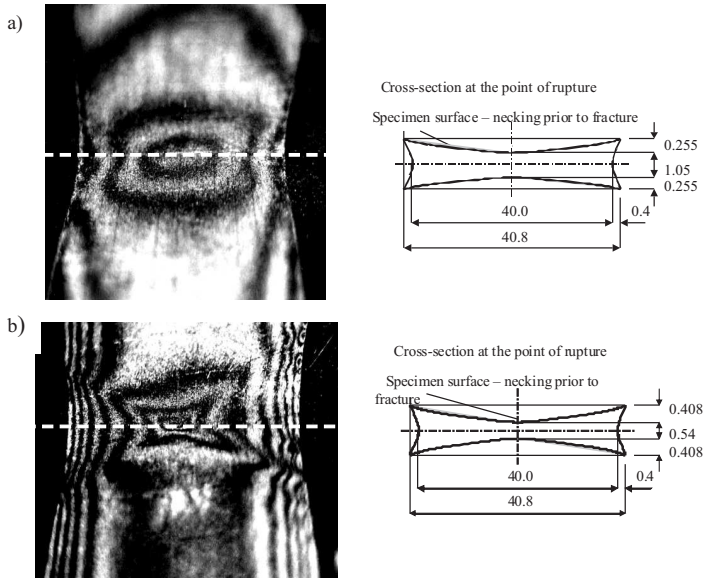

Figure 11 Distribution of the moiré-fringe patterns: a) occurrence of necking, b) prior to rupture on the surface (in the middle of the specimen) and changes in the cross-section at the point of rupture obtained with the moiré-fringe technique

The curves showing a variability of the stresses σ_β and σ_α and changes in the stress and strain intensities σ_{int} and ε_{int} , respectively, in the necking zone are plotted along the strain lines in bi-polar coordinates (Fig. 8) for various values of α along the curves β=const. (β=0, $\pi/24$, $\pi/18$, $\pi/16$, $\pi/12$,.. $\pi/4$) and in the form of surface functions $F(a_1,\alpha,\beta)$ (for two variables α and β). The changes in the specimen thickness calculated according to (35) were compared to the test results

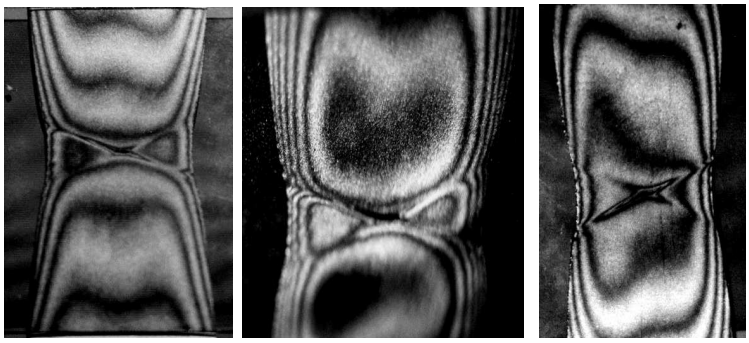

Figure 12 Distributions of the moiré-fringe patterns corresponding to an occurrence of the plastic strain zone, then fractures in the middle, and, consequently, the failure of the specimen

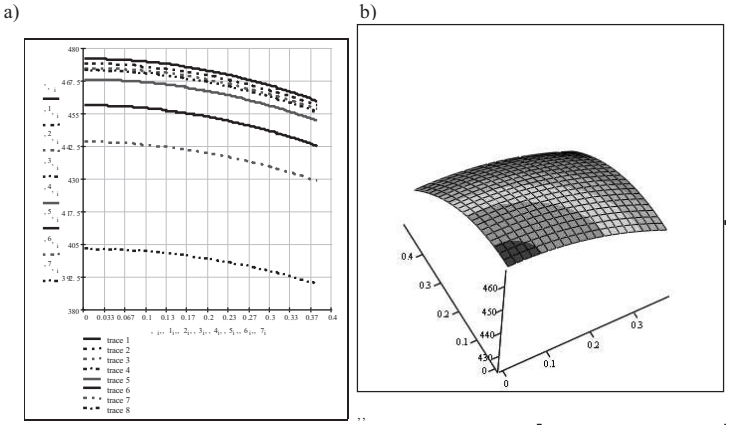

Figure 13 Distributions of the normal stresses $\sigma_\beta$according to formula (34) in the necking zone

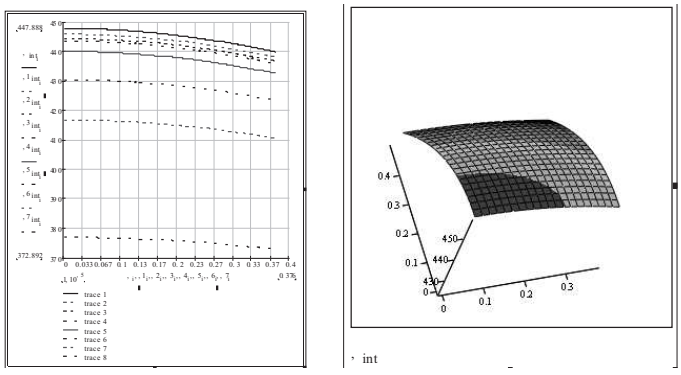

Figure 14 Distribution of the reduced stresses σ_{int} (stress intensity) according to the Huber hypothesis, according to formula (36)

obtained with the moiré-fringe technique.

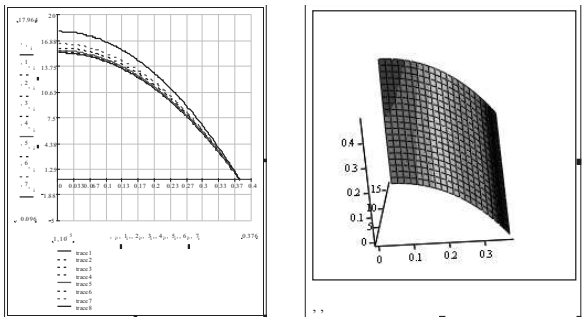

Figure 15 Distributions of the normal stresses σ_α according to formula (34) in the necking zone

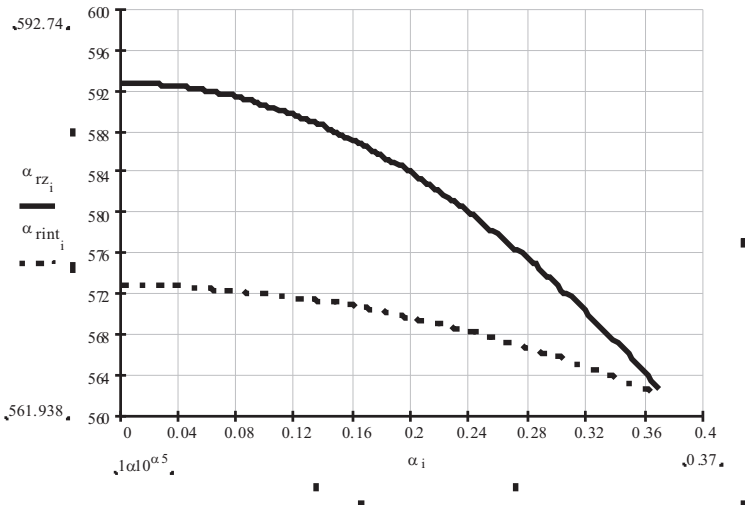

Figure 16 Distributions of the actual reduced stresses -σ_{int} (stress intensity) according to the Huber hypothesis and a comparison of values of mean and actual stresses

The distributions of strains prior to an occurrence of the central fissure (in the middle of the specimen) and strains on the specimen surface obtained with the moiré-fringe technique were compared to the calculation results. The differences in the measured and calculated changes in the specimen thickness Δh were equal to 2÷6 %.

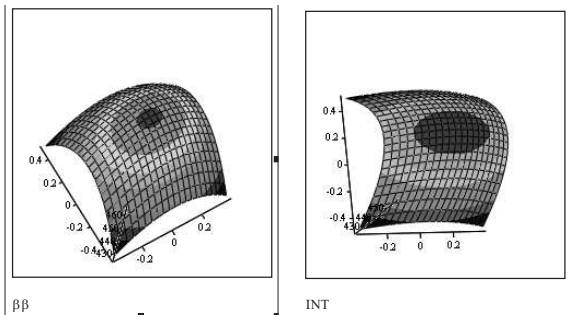

Figure 17 Distributions of the normal stresses σ_β and the reduced stresses -σ_{int} (stress intensity) according to the Huber hypothesis in the necking zone

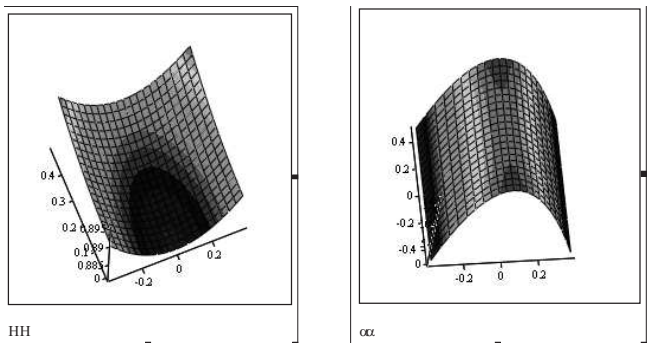

Figure 18 Changes in the specimen thickness Δh from the axis of symmetry. Distributions of the normal stresses σ_α in the necking zone

6. Zones of sliding lines (surfaces)

Under further loading, plastic strain zones and sliding lines (surfaces) start to occur and they can be described as a function of two variables x(α,β), y(α,β) on the basis of well-known relationships:

$$\frac{dy}{dx} = \pm\frac{2(\tau_{xy}-k)}{\sigma_y-\sigma_x} \quad \text{or :} \frac{dy}{dx} = \pm\frac{\sigma_y-\sigma_x}{2(\tau_{xy}-k)}, \quad \text{where: } k = \frac{\sigma_{int}}{\sqrt{3}} \tag{41}$$

The zones of plastic strains and sliding lines (surfaces) can be described on the basis of the main strain lines x(α,β), y(α,β), whereas the stress components have been calculated according to formulas (24) and (36)

1. Assuming that $\sigma_{int} = \sigma_\beta - \sigma_\alpha$ and $\tau_{xy} = \frac{\sigma_\beta-\sigma_\alpha}{2} \cdot \sin 2\varphi$
and $\sigma_y - \sigma_x = (\sigma_\beta - \sigma_\alpha)\cos 2\varphi$,

we obtain:

$$\frac{dy}{dx} = \pm\frac{\sigma_{int}\cdot\sin 2\varphi - 2k}{\sigma_{int}\cdot\cos 2\varphi} \quad \Rightarrow \quad \frac{dy}{dx} = \pm\left(tg2\varphi - \frac{2k}{\sigma_{int}\cdot\cos 2\varphi}\right) \tag{42}$$

After the integration:

$$y = \pm x\cdot\left(tg2\varphi - \frac{2k}{\sigma_{int}\cdot\cos 2\varphi}\right) + C_2 \tag{43}$$

where: $\sin 2\varphi = \frac{2 \cdot sh\alpha_i \cdot \sin\beta_i \cdot [(1+ch\alpha_i) \cdot \cos\beta_i]}{(ch\alpha_i + \cos\beta_i)^2}$ $\cos 2\varphi = \frac{2-(ch\alpha_i - \cos\beta_i)^2}{(ch\alpha_i + \cos\beta_i)^2}$

2. Assuming that plain stress occurs on the specimen surface, the intensity of stresses and strains have been calculated according to formula (36), and the sliding surface shape according to the following formula:

$$\frac{dy}{dx} = \pm \frac{\sigma_{int} \cdot \cos 2\varphi}{\sigma_{int} \cdot \sin 2\varphi - 2k}, \quad y = \pm x \cdot \left(\frac{\sigma_{int} \cdot \cos 2\varphi}{\sigma_{int} \cdot \sin 2\varphi - 2k} \right) + C_2 \tag{44}$$

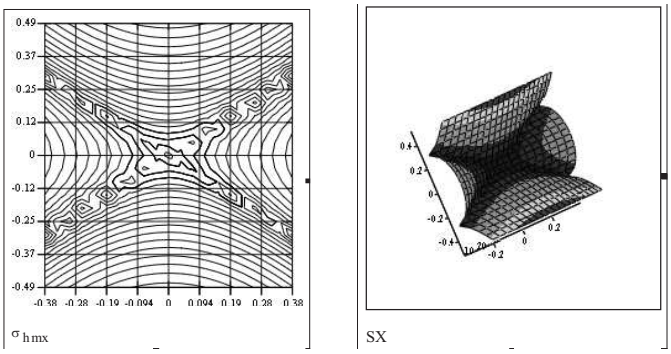

Figure 19 Zones of the plastic strains and the sliding lines (surfaces) at the point of necking prior to fracture, calculated according to (43)

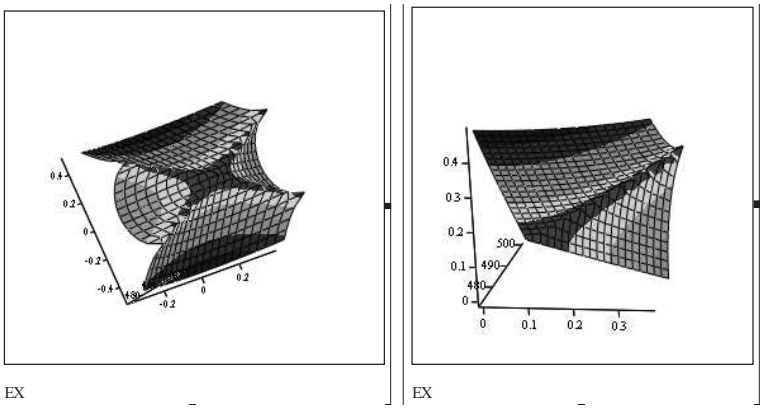

Figure 20 Distributions of the reduced stresses according to the Huber hypothesis along the sliding line at the point of necking prior to fracture, calculated according to (44)

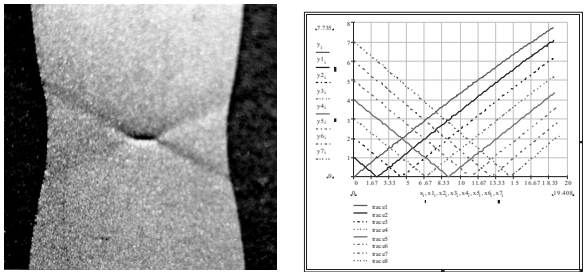

Figure 21 Specimen surface in strain and the sliding lines, calculated according to (43). Due to the two-axis symmetry, $^1/_4$ of the specimen has been presented at the point of necking

7. Results of numerical calculations of the specimen under test

The results of experimental investigations and calculations have been compared to the results of numerical calculations (with the finite element method, using the ANSYS 6.1 software package). In the model for numerical calculations, the dimensions such as in the initial phase of necking have been assumed. (Fig. 6). The material properties $\sigma(\varepsilon)$ assumed in the computations in the form of a polygonal curve correspond to actual stresses and strains at the point of necking (Fig. 22).

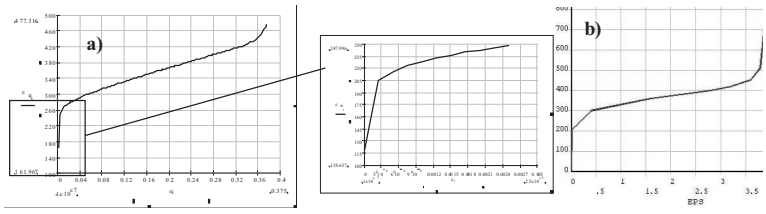

Figure 22 Material properties $\sigma(\varepsilon)$: a) obtained from the tests, b) assumed in the FEM computations

8. Conclusions following from the tensile test

The conducted tests and numerical calculations of the tensile test are aimed at the verification of the mathematical model that can be applied in further computations. The presented formulae enable a description of stresses in the whole range of loading, taking into account necking and a determination of the intensity of stresses, a description of the generation of the sliding lines, or strictly speaking, the sliding surfaces.

The way the strains have been described in bi-polar coordinates, which has been based on experimental investigations, allows for employing the results into numerical calculations, where we are interested in stress states in failure. The description of

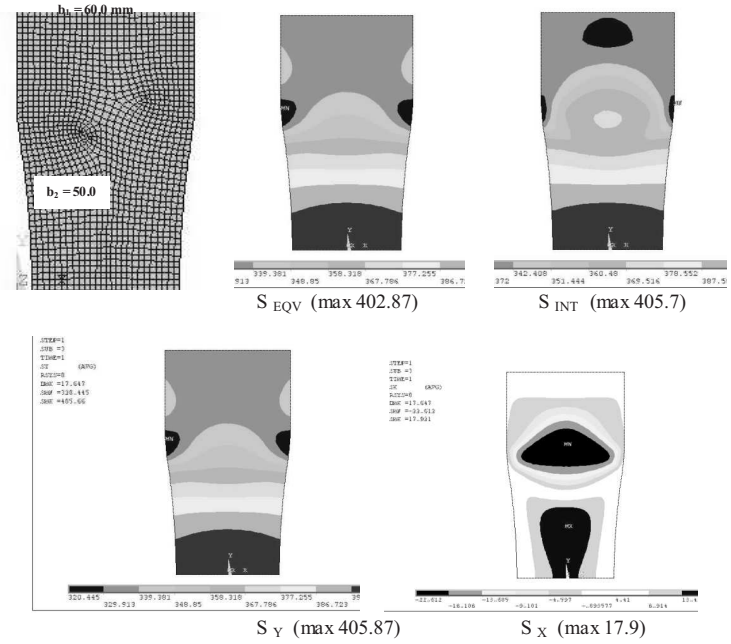

Figure 23 Results obtained on the basis of the FEM numerical calculations (ANSYS 6.1). The drawings show: a mesh of elements, distributions of the reduced stresses according to the Huber hypothesis and distributions of the maximum shear stresses τ_{max}, distributions of the normal stresses σ_y and σ_x

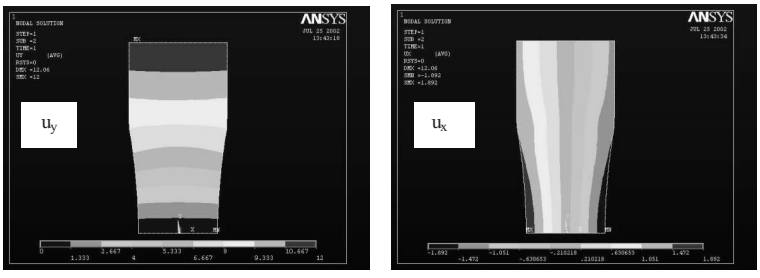

Figure 24 Results obtained on the basis of the FEM numerical investigations (ANSYS 6.1). The distributions of the displacements u_y and u_x are shown

the stress-strain relationship, which takes into account strain hardening and necking under rupture and the determination of the magnitude of breaking stresses, makes it possible to develop a numerical model until the element failure occurs. The distributions of strains calculated according to the presented formulae are convergent with the results of strain tests in the neighbourhood of necking.

The simplified analysis of the stress state in bi-polar coordinates can be used to build a numerical model if we assume a division of the specimen into two basic elements: a part that is subjected to uniform tension (L_{01}) and a part that has

been subjected to uniform tension and then necking (L_{02}).

The scheme of failure can be described as follows: the value of the maximum force obtained during the tensile test and the strain corresponding to it enables a determination of the parameter or the function of strain hardening. In order to obtain the maximum force, we can assume uniform tension, then the necked part is subject to strain as a matter of fact.

While analysing the test results, the following should be defined:

1. strains corresponding to the limit of proportionality and to the yield point,
2. strains corresponding to the maximum tensile force,
3. strains corresponding to necking at the instant of rupture and the dimensions of the cross-section.

Next, an influence of necking, at which an increase in stresses and a rupture of the material cohesion forces take place and a fracture (a vertical central fissure propagating symmetrically along the sliding lines) occurs, and then the material breaks along the sliding line, should be considered.

The sliding lines determined experimentally and analytically in the failure phase go at the angle of 60° with respect to the vertical axis, and not at the angle of 45° as has been assumed in numerous theoretical solutions.

A good agreement between the FEM numerical results (ANSYS 6.1) and those obtained from the tests has been found. Because of too little a number of tests, one cannot draw too explicit conclusions, nevertheless the presented actual $\sigma - \varepsilon$ (stress-strain) relationship in the whole range of loading makes it possible to employ the mathematical model that can be applied in further material strength calculations.

References

[1] **Bridgman P W**: *Studies in large plastic flow and fracture*, Mc Graw - Hill, New York 1952.

[2] **Cherepanov G. P.**:*Mechanics of brittle fracture*, Mc Graw - Hill, New York 1979.

[3] **Frocht M. M.**:*Photoelasticity*, John Wiley, New York 1960.

[4] **Hill R.**:*The mathematical theory of plasticity*, Oxford: The Clarendon Press 1950.

[5] **Hoffman O., Sachs G.**:*Introduction to the Theory of Plasticity for Engineers*, McGraw- Hill Book Company, Inc. 1953.

[6] **Kobayashi A. S., Harris D. O., Engstrom W. L.**:*Transient Analysis in a Fracturing Magnesium Plate*, Experimental Mechanics, 1967.

[7] **Ludwik P.**:*Elemente der technologischen Mechanik*, Berlin: Springer 1909.

[8] **Mróz Z.**:*Non- associated flow laws in plasticity*, *Journal de Mecanique*, **2**, 1963.

[9] **Sih G. C.**:*Hanbook of Stress-Intensity Factors*, Bethlehem, Leigh University Press, **1**, 1973.

[10] **Sih G. C.**:*Strain-energy-density factor applied to mixed mode crack problems*, *Int. J. of Fraction*, **10**, 305-321, 1974.

[11] **Sih G. C., Hutchinson J.**:*Fully Plastic Solutions and Large Scale Yielding Estimates for Plane Stress Crack Problems*, *Journal of Engineering Materials and Technology*, **76**, 1976.

[12] **Tada H., Paris P., Irwin G. R.**:*The stress analysis of cracks: Handbook*, Hellertown: Del Research Corp. 1973.

[13] **Timoschenko S.**:*Theory of Elasticity*, John Wiley, New York 1980.

[14] **Tvergaard V. and Hutchinson J. W.**:*Effect of strain-dependent cohesive zone model on prediction of crack growth resistance*, *Int. J. Solid Structures*, **33**, 3297-3308, 1996.

[15] **Tetelman A. S. , Wilshaw T. R. and Rau C. A.**:*The critical tensile stress criterion for cleavage*, *Int. Journal of Fracture Mechanics*, **4**, 1968.

[16] *User's Guide ANSYS(2002): 6,9*, Ansys, Inc., Huston, USA.

[17] **Wegner T.**:*Surface of limit state in nonlinear material and its relation with plasticity condition*, *The Archive of Mechanical Engineering*, **3** XLVII, 205-223, 2000.

[18] **Wegner T.**:*A method of material modelling with the use of strength hypothesis of inner equilibrium stability*, *Mechanics and Mechanical Engineering*, **2** 4, 139-147, 2000.

[19] **Zienkiewicz O. C.**:*The Finite Element Method in Engineering Science*, Mc Graw - Hill, London, New York 1971.